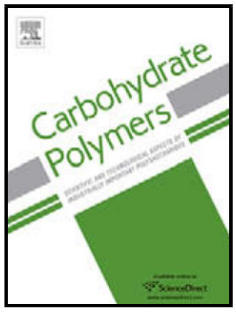

Title: Ultrasonication of insulin-loaded microgel particles produced by internal gelation: impact on particle's size and insulin bioactivity

Author: Ana C. Santos Joana Cunha F. Veiga A. Cordeiro-da-Silva Antonio J. Ribeiro

PII: S0144-8617(13)00659-0
DOI: http://dx.doi.org/doi:10.1016/j.carbpol.2013.06.063
Reference: CARP 7881

To appear in:

Received date: 3-12-2012
Revised date: 13-6-2013
Accepted date: 27-6-2013

Please cite this article as: Santos, A. C., Cunha, J., Veiga, F., Cordeiro-da-Silva, A., & Ribeiro, A. J., Ultrasonication of insulin-loaded microgel particles produced by internal gelation: impact on particle's size and insulin bioactivity, *Carbohydrate Polymers* (2013), http://dx.doi.org/10.1016/j.carbpol.2013.06.063

Ultrasonication of insulin-loaded microgel particles produced by internal gelation: impact on particle's size and insulin bioactivity

Ana C. Santos[a], Joana Cunha[b,c], F. Veiga[a], A. Cordeiro-da-Silva[b,d], Antonio J Ribeiro[a*]

[a] Centro de Estudos Farmacêuticos, Faculty of Pharmacy, University of Coimbra, Pólo das Ciências da Saúde, Azinhaga de Santa Comba, 3000-548 Coimbra, Portugal
[b] IBMC - Instituto de Biologia Molecular e Celular, University of Porto, 4150-180 Porto
[c] Institute for the Biomedical Sciences Abel Salazar and Faculty of Medicine, University of Porto, 4050-343 Porto, Portugal
[d] Faculty of Pharmacy, University of Porto, 4050-343 Porto, Portugal

*Correspondence to: António J Ribeiro (Telephone: +351-239488400; Fax: +351-239488503; E-mail address: aribeiro@ff.uc.pt)

ABSTRACT

Alginate-dextran sulfate (ADS) microgel has been used to protect insulin from gastrointestinal attack and as a carrier to promote insulin permeation through intestinal epithelium. The throughput of ADS submicron particles generation by emulsification/internal gelation is limited by its wide size distribution.

ADS: alginate/dextran sulfate
NPs: nanoparticles
LD: laser diffractometry
CD: circular dichroism
DMEM: dulbecco's modified eagle medium
FBS: fetal bovine serum
Cryo-SEM: cryo-scanning electron microscopy
ANOVA: one way analysis of variance
LOD: limit of detection
DLS: dynamic light scattering
ELS: electrophoretic light scattering
PI: polydispersity index
w/o: water/oil

The aim of this work was to study the recovery protocol influence on ADS particles through the determination of its impact on particles' size distribution and bioactivity. ADS particles showed a wide and multimodal distribution, characterized by a high aggregation phenomenon. In an attempt to reverse particles' tendency to aggregate and to homogenize particle size ADS populations were submitted to ultrasonication, while particle size distribution, physical and chemical stability, and the bioactivity of entrapped insulin were investigated. After ultrasonication a narrower particle population shifted to the nanoscale, with higher physical stability and significant insulin bioactivity was obtained. Emulsification internal/gelation followed by ultrasonication constituted a valid strategy to obtain ADS particles at the submicron range, with high stability and without significantly compromising insulin bioactivity, so offering promises, under previously well established conditions, to evaluate impact of ADS particle's size on biopharmaceutical and pharmacokinetics phases.

KEYWORDS: hydrogels; particle size; physical stability; ultrasound; emulsion; *In vitro* models.

1. Introduction

Microgels have gained considerable attention in recent years as one of the most promising nanoparticulate drug delivery systems owing to their unique potentials via combining microgel's hydrophilicity and extremely high water content with a nanosize scale. Particles' size is a keyrole in biomedical applications, with given influence on biorecognition (Hwang, Truong & Sim, 2012), biodistribution (Hirn et al., 2011), bioadhesion (Hasani, Pellequer & Lamprecht, 2009), biocompatibility (Akbar, Mohamed, Whitehead & Azzawi, 2011), and biodegradation (Cui, Hunter, Yang, Chen & Gan, 2011). Smaller particles may penetrate cells by passing directly through the cell membrane or infiltrate between cells, translocate to new sites and to the blood/lymph and thereby target organs away from their portal of entry (Geiser et al., 2005). Controlled release experiments with hydrophobic dexamethasone and hydrophilic vitamin C used as encapsulant models showed that for these small molecular drugs, the loading amount was mainly determined by the surface area of the nanoparticles (NPs), and the subsequent release of the drug dramatically decreased with the increasing of the particle size (Gan et al., 2012). Therefore, emulsification/internal gelation technique, initially conceived for microparticles preparation (Poncelet, Lencki, Beaulieu, Halle,

Neufeld & Fournier, 1992), rapidly spurred interest in extending it into the submicron range.

Recent works concerning insulin delivery systems have shown good characteristics in terms of insulin chemical stability and bioactivity maintenance (Luo et al., 2012; Zhang et al., 2010), however most of them are for subcutaneous injection (Al-Tahami, Oak & Singh, 2010; Chen, Wu, Guo, Xin & Li, 2011; Oak & Singh, 2011) and use synthetic instead of biopolymers. Insulin-loaded alginate-dextran sulfate (ADS) particles prepared by emulsification/internal gelation constitute a promising controlled delivery system for oral route (Reis, Veiga, Ribeiro, Neufeld & Damge, 2008). The objective of insulin entrapment into the polymeric matrix is to minimize protein denaturation, stabilizing and maintaining its physiological activity during both particle manufacturing and drug release (Reis, Ribeiro, Houng, Veiga & Neufeld, 2007; Silva, Ribeiro, Figueiredo, Goncalves & Veiga, 2006), namely in the passage through the stomach in order to enhance its bioavailability (Krishnankutty, Mathew, Sedimbi, Suryanarayan & Sanjeevi, 2009).

ADS submicron particles generation by emulsion and internal gelation is a scalable method of encapsulation and is based on the release of calcium ion from an acid soluble calcium salt in emulsified ADS solution. This is achieved by acidification with an oil-soluble acid, which partitions to the dispersed aqueous alginate phase, releasing soluble calcium and initiating gelation.

One of the limitations of this technique lies in the ability to obtain monodispersed particles' populations. ADS particles showed polydispersed populations, characterized by a wide distribution of size values which derive from nano- and microparticles and also aggregates coexistence (Reis, Ribeiro, Houng, Veiga & Neufeld, 2007; Reis, Veiga, Ribeiro, Neufeld & Damge, 2008), which is characteristic of emulsification methods using biodegradable polymers (Gaumet, Gurny & Delie, 2009). Moreover, the reduced size of particles together with their large surface area, can lead to particle-particle aggregation during storage and transportation of particle dispersion.

ADS particles were successfully produced by emulsification/internal gelation and recovered by using a washing medium composed of acetate buffer pH 4.5/isopropanol/acetone/hexane coupled to centrifugation (Reis, Ribeiro, Neufeld & Veiga, 2007). Even though these solvents levels were below the limits accepted in the pharmaceutical field for collected particles, a recovery protocol with no solvents or with the minimum use of them is an increasing value of the technique. Acetate buffer

contributes to retain insulin in NPs network while the use of solvents aims to collect microgel from biphasic medium. Acetone is indispensable due to its low viscosity and also its miscibility with both aqueous phase and the predominant hydrophobic emulsion phase medium, conferring high mobility to the particles and allow a successful particles' recovery.

The first concern in ADS particles produced by the present method is the necessity of an approach to size-fraction particles' populations, to obtain a more detailed description and better understanding of these particles. To attain this aim, a recovery protocol of microgel particles, based on the coupling of centrifugation and acetone as washing medium was used. Whether ultrasonication can disaggregate collected microgel while keeping insulin bioactivity was investigated. Physical stability was determined through sedimentation tests and zeta potential; and chemical stability was evaluated using circular dichroism (CD) and HPLC-MS analysis. Submicron particles with a narrow size distribution, with high insulin content, retention of insulin bioactivity and good physical and maintained chemical stability were aimed.

2. Materials and methods

2.1. Materials

Sodium alginate (viscosity of 2% solution at 25°C, 250cps) extracted from *brown algae*, dextran sulfate (5kDa), Victoria-blue R and Phosphotungstic acid, Sorbitane monooleate (Span 80®) were purchased from Sigma-Aldrich (Steinheim, Germany). Ultrafine calcium carbonate (Setacarb 06 calcium) was supplied from Omya (Organ, France). Insulin (Actrapid® Insulin) was kindly donated from Hospitais da Universidade de Coimbra – Coimbra, Portugal, supplied by Novo Nordisk (Bagsvaerd, Denmark). Paraffin oil was purchased from Fagron (Terrasa, Spain). Dulbecco's Modified Eagle Medium (DMEM), fetal bovine serum (FBS), L-glutamine and Penicilin/Streptomycin were purchased from Lonza (Visp, Switzerland). 10x solution of trypsin-EDTA was prepared from porcine trypsin and EDTA powders obtained from Sigma-Aldrich (Steinheim, Germany). Paraformaldehyde was purchased from Merck (Darmstadt, Germany). A Thermo Scientific Pierce® BCA Protein Assay Kit was obtained from Thermo Scientific (Rockford, Illinois, USA). Fast-activated cell based AKT (FACE-AKT) ELISA kits were manufactured by Active Motif (Carlsbad, California, USA) and purchased from Frilabo (Maia, Portugal). All other reagents were of analytical grade and were used as received.

2.2. Methods

2.2.1. Preparation of alginate-dextran sulfate particles

ADS particles were prepared according to an adaptation from the emulsification/internal gelation technique previously described (Poncelet, Lencki, Beaulieu, Halle, Neufeld & Fournier, 1992). An aqueous solution of low viscosity sodium alginate (2%, w/v) and dextran sulfate (0.75%, w/v) was prepared by orbital shaking. Insulin (100 IU/mL, 10mL) was mixed into ADS solution. An aqueous suspension of calcium carbonate (5%, w/v) was sonicated for 30 min and then it was dispersed into the ADS-insulin solution (calcium-alginate ratio, 7%, w/w). The resulting mixture was emulsified within paraffin oil with sorbitane monooleate (1.5%, v/v) by impeller-stirring homogenization (1600 rpm, 30 min). Gelation was triggered *in situ* by the dissolution of calcium complex, as a consequence of the addition of 20 mL of paraffin oil containing glacial acetic acid (molar ratio acid-calcium, 3.5) during 15 min, with continued stirring. Unloaded particles were prepared as controls. Each batch was prepared in triplicate.

2.2.2. Particle recovery

Oil-dispersed ADS particles were recovered through an extraction with a medium consisting of acetone with acetate buffer (pH 4.5) (1:10, v/v) (USP 30-NF 25). ADS particles were subjected to extra washing cycles consisting of coupling washing medium extraction/centrifugation until no more oil was found under microscopic observation. These particles were stored at 4°C in acetate buffer.

2.2.3. Morphological analysis

Morphology of hydrated particles stained with Victoria-blue R was monitored by optical microscopic observation using an optical microscope equipped with a Digital Sight DS-U2 microscope camera controller. The shape and surface and mass spectroscopy of hydrated particles were analysed by Field Environmental (FE)-Cryo-SEM with EDS-JEOL JSM 6301F scanning microscope (Oxford INCA Energy 350, Gatan Alto 2500). Phosphotungstic acid-stained particles were frozen using liquid nitrogen slush (-210 °C) under vacuum, to allow their fracture in order to obtain a fresh and clean surface for examination. After that, samples were sublimated at -90°C for 4 min to remove top layers of water molecules. Finally, samples were sputter coated with gold/palladium for 40 seconds, followed by image capturing.

2.2.4. Determination of Recovery Yield

Recovery yield of the process was assessed by measuring the ratio between isolated particles and total recovered particles (v/v), according to the following equation Eq. (A):

Recovery Yield (%) = (*Volume of isolated particles*/*Total recovered particles*)×100 (A)

2.2.5. Determination of Insulin Content

Insulin was extracted from particles firstly by treatment with sodium citrate 2M (1/2, v/v) followed by orbital shaking. Insulin concentration was determined using Pierce® BCA Protein Assay Kit. Unloaded particles were used as control and assay was performed in triplicate. Calibration curve was made using different concentrated solutions of insulin in the same medium. Insulin content (%) was assessed according to the equation below Eq. (B):

Insulin Content (%) = (Insulin mass in isolated particles/Total recovered insulin mass) × 100 (B)

2.2.6. Particle size analysis

Size distribution analysis was performed by laser diffractometry (LD) using a laser diffraction particle size analyser (Beckman Coulter® LS 13 320, Miami, FL, USA) with polarization intensity differential scattering (PIDS). The real refractive index and the imaginary refractive index were set to 1.36 and 0.01, respectively. Three measurements of 90s were used to obtain the LD data, which were expressed using volume distributions, and given as diameter values corresponding to percentiles of 10%, 50% and 90%, using the Mie theory. The span value is a statistical parameter useful to characterize the particle size distribution, which is obtained through the following equation (Wissing, Kayser & Muller, 2004):

Span = (*d*90%−*d*10%) / *d*50%.

The particle size of selected samples was additionally investigated by dynamic light scattering (DLS) using other particle size analyser (DelsaNano C, Beckman Coulter Delsa™). Mean diameter, size distribution and polydispersity index (PI) (which

measures the width of the size distribution) of pH 4.5 buffered particle's suspensions were determined in triplicate at 25°C with an angle measurement of 60°. Previous measurement, the dispersions were diluted with acetate buffer to an appropriate concentration of particles to avoid multiple scattering before. One measurement was performed after an equilibration period of 3 min for 300 s at 25°C to obtain the results. Both instruments were routinely checked and calibrated using standard latex particle kit (Beckman Coulter, Inc.).

2.2.7. *In vitro* release studies

In vitro release behavior was assayed by incubating 5 mL of ADS particles suspension in 5 mL of HCl buffer at pH 1.2 (British Pharmacopoeia, 2010), under magnetic stirring (100 rpm, 2 h), simulating stomach conditions without enzymes under sink conditions. To simulate the progress of particles moving from the stomach into the upper small intestine, the buffer was changed to higher pH after 2 h min. Particles were centrifuged (12500 g, 10 min), then resuspended in 10 mL phosphate buffer at pH 6.8 (British Pharmacopoeia, 2010)), under magnetic stirring (100 rpm) during 10 h. Samples at appropriate intervals were withdrawn and replaced by the same volume of fresh incubation medium, and were assayed for insulin content in the supernatant after centrifugation (12500 g, 10 min), using Pierce® BCA Protein Assay Kit. All the operations were made in triplicate.

2.2.8. Ultrasonication exposure

Ultrasonication was applied with Ultrasonicator Sonics® VCX130 (Sonics & Materials, USA) for two five-minute cycles with 52W, after dilution of 10 mL of ADS particles into 1:1 with acetate buffer, in order to obtain a narrower ADS particles' population. The temperature was controlled around 25°C by using an ice bath.

2.2.9. Zeta potential analysis

Zeta potential measurements, which reflect the electric charge on the particle surface, were taken by electrophoretic light scattering (ELS) using a Nano Zeta Potential Analyser (DelsaNano C, Beckman Coulter Delsa™). Measurements were taken in a Flow Cell (Beckman Coulter Delsa™) at 25°C and acetate buffer solution pH 4,5 was used as diluent to proper concentration. Zeta potential values are presented as means of triplicate runs per sample. The instrument was routinely checked and calibrated using mobility standard (Beckman Coulter, Inc.).

225

226 **2.2.10. Sedimentation tests**

227 In sedimentation tests, an analytical centrifugation system detects the intensity of
228 transmitted light over the entire sample length as function of time and position, while
229 the sample was being centrifuged (Lerche, 2002). Accelerated physical stability testing
230 of ADS particles was performed using a LUMisizer® (L.U.M. GmbH, Germany)
231 centrifuge, working at 2000 rpm, during 128 min and 25ºC, which measured the
232 transmission variations of particles' suspensions under centrifugation against time. All
233 data were stored and displayed in real time as a function of radial position, enabling
234 analysis of the dispersion characteristics.

235

236 **2.2.11. Insulin bioactivity *in vitro* assay**

237 NIH/3T3 fibroblast cell line was cultivated in DMEM with 4.5 g/L glucose
238 supplemented with 10% heat inactivated FBS, 2mM L-glutamine, 100 U/mL penicillin,
239 100 U/mL streptomycin. The cells were passed 1:4 twice a week at 80% confluence
240 with 0.05% trypsin-0.02%EDTA. To prepare the cells for the FACE^{TM} AKT assays the
241 fibroblasts were trypsin-released, washed, and counted with a hemocytometer with
242 trypan blue viability staining. The cells were seeded in flat-bottom, tissue culture treated
243 96-well plates at a density of $3.5x10^4$ cells/well in 200µL of complete medium. Two
244 identical plates were prepared, one to measure AKT phosphorylation and the second for
245 the assessment of the total AKT protein under the same conditions. The plates were
246 incubated overnight (37 ºC/5% CO_2) to achieve 80% confluence. Prior to stimulating
247 the cells with insulin, the medium was aspirated and the cells were washed twice with
248 PBS. The cells were then incubated (37 ºC/5% CO_2) in serum-free starvation medium
249 (DMEM with 4.5 g/L glucose, 2 mM L-glutamine, 100 U/mL penicillin, 100 U/mL
250 streptomycin) for 8h. Subsequently, the cells were exposed to either: (i) active, free
251 insulin or (ii) insulin released from the ADS particles (into sodium citrate 2M, as
252 described before for insulin determination content assay). The samples were then
253 diluted to 150nM in starvation medium based on the total protein content measured
254 using UV absorbance, as described previously. Blank particles without insulin, treated
255 identically, were used as negative controls. For each trial, a standard curve was prepared
256 using free insulin with concentrations ranging from 50-200 nM in starvation medium
257 and citrate buffer adjusted to the percentage equivalent to the volume inherent to the
258 samples. The cells were stimulated for 10 min with 200 µL of the insulin-containing

samples applied to each well. At the end of the stimulation period, the medium was aspirated and the cells were immediately fixed in 4% paraformaldehyde in PBS. The plates were incubated at room temperature for 20 min and stored at 4 ºC until the next step of the assay. Insulin bioactivity was determined by quantifying the ratio of p-AKT protein to total AKT protein using the FACE^{TM}-AKT immunoassay, normalized to the total cell count, according to the manufacturer's instructions, and interpolated into the standard curve. Briefly, the fixed cells were washed 3 times in washing buffer and incubated overnight at 4 ºC in primary antibody solution specific for p-AKT or total AKT. After 3 washing steps, the HRP-conjugated anti-rabbit IgG was applied for 1 h, following which the substrate/developing solution was added to initiate the colorimetric reaction. After 20 min, the stop solution was added and the absorbance was measured at room temperature using a plate reader spectrophotometer (Synergy 2 Multi-Mode Microplate Reader, Biotek) at 450 nm corrected by the absorbance at 655 nm. For each sample, the absorbance data for both p-AKT and total AKT were normalized to the total cell number per well by staining with crystal violet and measuring the absorbance at 595 nm. After normalization to the total cell count, the ratio of p-AKT to total AKT was calculated for each sample condition as a measure of the extent of activation of the AKT pathway by the insulin. Negative controls without the primary antibody were included in every trial to ensure the binding specificity. Insulin bioactivity was quantified by the ratio between phosphorilated and total AKT, on a per cell basis, expressed in percentage after incubation with the insulin released from ADS particles, as manufacture instructions.

2.2.12. Circular Dichroism Spectroscopy

Secondary structure of the released insulin from ADS particles before and after ultrasonication, as well as fresh standard insulin, was evaluated using CD. CD spectra were obtained with a Jasco J-720 spectropolarimeter (Tokyo, Japan) equipped with a temperature controller to examine the secondary structure of insulin in particles. Spectra were collected at 25°C using a 0.2 cm cell over the wavelength range of 200–260 nm. A resolution of 0.2 nm and scanning speed (50 nm/min) with a 4 s response time were employed. Each spectrum obtained represents an average of five consecutive scans. Noise reduction, blank buffer subtraction, and data analysis were performed using standard analysis and temperature/wavelength analysis programs (Jasco). Samples for

CD analysis were prepared by dissolution in isotonic PBS buffer (British Pharmacopoeia, 2010). The spectra of insulin samples with concentrations about 5 μM were compared with that of fresh insulin in the same medium.

2.2.13. HPLC-MS

HPLC-MS was used to investigate the chemical stability of released insulin from ADS particles throughout production, particles recovery and ultrasonication procedures. Samples were analyzed using a Liquid Chromatography of High Performance (Thermofinnigan) coupled to a quadrupole *Ion Trap* Mass Spectrometer (QIT-MS) system (LCQ, Advantage Max, Thermofinnigan, San Jose, CA), with an electrospray ionization (ESI) interface operated in the positive-ion mode. A C18 Reversed Phase column (150 × 2.1 mm; particle size: 3 μm; Waters Spherisorb ODS2) and a Guard Cartridge (4.6 × 10 mm; particle Size: 5 μm; Waters Spherisorb ODS2), kept at a temperature of 27˚C, were used for the separation.

The mobile phase was composed by water (0.04% v/v trifluoroacetic acid):acetonitrile (0.04% trifluoroacetic acid), 80:20 v/v at a flow rate of 500 μL/min. A linear gradient of 20%–40% (acetonitrile 0.04% v/v trifluoroacetic) over 10 min was performed. An injection volume of 25 μL of the samples was considered for the analysis.

An insulin standard solution was prepared and considered as reference. Insulin samples for HPLC-MS analysis were prepared by dissolution in citrate sodium 55 mM prior to analysis. The XCALIBUR software package (Thermofinnigan) was used for data acquisition and analysis.

2.2.14. Statistical Analysis

Statistical analysis was performed using SPSS® Statistics (version 19, IBM® SPSS®). Size percentiles, mean particle size, zeta potential, recovery yield, insulin content and insulin bioactivity were represented using sample mean ± standard deviation (SD). Normality of the distributions of these variables was verified using Shapiro-Wilk test. Comparison between ultrasonication cycles was performed using one way analysis of variance (ANOVA). *Post hoc* comparisons were obtained using Tuckey's test. Comparisons between insulin-loaded and unloaded conditions were obtained using student's t test for independent samples when the underlying distribution was considered normal; Mann-Whitney's test was used in the other situation. A significance of 0.05 was considered throughout the analysis.

3. Results and Discussion

ADS particles were prepared by emulsification/internal gelation, which comprises the formation of an emulsion and internal gelation using high stirring speed. However, producing microgel with desired properties (especially narrow submicron size distribution with high encapsulation efficiency) is still a challenge. Several factors could affect size of microgel particles obtained by emulsification namely stirring speed, viscosity of both internal and external phases and recovery protocol. Characterization of collected particles was made in relation to macroscopic features, recovery yield and insulin content. ADS particles showed that after rest at 4°C, they showed gel-like precipitate characteristic aspect, due to their high water content, according to their biopolymeric nature.

The analysis and discussion of recovery yield, insulin content and particle size distribution will be done below. Further, the impact of ultrasonication on ADS particles will be evaluated in terms of size distribution, in physical stability by potential zeta measurements and sedimentation tests, and also in insulin bioactivity through *in vitro* studies.

3.1. Recovery Yield

Extraction medium use coupled to centrifugation as recovery protocol, to attempt the extraction of ADS particles from the biphasic medium to the aqueous phase, was found to be around 50% and thus beneficial in terms of recovery yield (namely 49±14% and 53±11% for insulin and unloaded particles respectively, with no significant difference). Remaining particles, not considered for this study, were collected only by the gravitational force, corresponding to the higher-sized particles and macroscopically visible aggregates. High recovery yield obtained with actual recovery protocol can be explained by the efficiency of the applied recovery medium and centrifugation force to remove particles from biphasic medium. This is especially important to the lower-sized particles, especially the desired submicron and NPs, which offer more difficulties to recover and to maintain segregated, within a polydisperse population characteristic of biopolymeric particles. Acetone/acetate buffer in 1:9 (v/v) as particles washing medium didn't trigger any structural particles' changes, like shape alterations confirmed by Cryo-SEM microphotographs (data not shown), whilst that occurred when a higher acetone proportion 4:6 (v/v) was used (Reis, Ribeiro, Neufeld & Veiga, 2007).

3.2. Insulin Content

Recovery protocol allowed obtaining around 57±6% of encapsulated insulin, lower than those reported previously (Reis, Ribeiro, Veiga, Neufeld & Damge, 2008). Insulin losses could have been due to particles' stress during either their preparation or recovery. Firstly, during washing used to remove residue oil from the particles surface, insulin may has been drawn out of the particles following the extracted water, in which process probably smaller particles were more affected. Secondly, centrifugal force effect may have contributed also for insulin losses, due to porous nature of ADS particles. In the other hand, the presence of acetone may have caused some diffusive loss of encapsulated insulin owing to its dehydrating effect. Thus, the balance between insulin retention inside microgel and water extraction or/and centrifugal force use must be considered.

3.3. Size characterization (before and after ultrasonication cycles)

During recovery of ADS particles, the appearance of aggregates was macroscopically observed. Aggregation is very common during nanoencapsulation especially when hydrophilic particles are obtained by emulsification. The higher stirring speed used to reduce mean particle diameter in the manufacture process causes a distribution of turbulent forces throughout the emulsion, which contributes to a higher heterogeneity of emulsion and consequently final microgel particles, resulting in particles with a wider distribution in size (Silva, Ribeiro, Figueiredo, Ferreira & Veiga, 2005). During emulsification and before gelation, samples were taken and observed under light microscopy and microphotographs showed emulsion droplets sizing higher than 1000 nm and no existence of aggregation, as illustrated in Fig. 1. After that, and before recovery from biphasic medium, ADS particles prepared by emulsification/internal gelation remained spherical and discrete but some particles larger than 1000nm and aggregates were formed (data not shown).

On the other hand, insulin (pI≅5.4) and both alginate and dextran sulfate show opposite charges, allowing interaction through electrostatic interactions. These physical surface charges contribute to particles' network; however they do contribute also to aggregation, owing to their great affinities. Aggregation was potentiated also due to particle adhesion, especially under van der Waals forces (Nguyen, Rouxel, Hadji, Vincent & Fort, 2011).

Recovery medium, composed by acetate buffer and acetone, promoted high mobility to larger particles and aggregates primarily recovered by sedimentation. Particles dispersed in the remaining biphasic medium were theoretically smaller, and thus more difficult to extract. Centrifugation force applied to particles recovery in the presence of the washing medium could allow the recovery of the remaining and lower size particles of the biphasic medium. As the composition of the washing medium used in the washing cycles to remove the residual oil before the recover protocol was constant among recovery cycles, aggregation seemed to be triggered by aftermost particle handling conditions.

Size distribution of insulin particles is shown in Fig. 2(a) in terms of volume. Insulin diameter values corresponding to percentils of 10%, 50% and 90% and also span value are depicted in Table 1. Regarding ADS particles' size distribution, it was divided into two ranges: one range was constituted of NPs and low-sized microparticles (< 4 μm), and the main range was constituted of higher-sized microparticles (d90% = 144.8±30.45 μm). Therefore, unloaded particles, after recovery, showed a wide size distribution as expected, with the predominant percentage of microparticles probably due to the presence of aggregates and a lower percentage of low-sized particles (Table 1).

As it had been said before, particles' size-fractioning using recovery medium coupled to centrifugation promoted enhancement of particles extraction from biphasic medium, indicated by a significant recovery yield percentage value (~50%). However, it can probably simultaneously had contributed to parallel aggregation phenomena due to high ultracentrifugation forces.

With respect to percentage of smaller particles, namely within nano- and submicron range (<1000nm), it was possible to observe through the values of percentils a large increase between d10% (364 ±124 nm) and d50% (26.16±3.89 μm) values, exposing the existence of a very low percentage of low-sized particles, according to size distribution analysis, which reinforces the obstacle in obtaining and recovering discrete submicron microgel particles by emulsification. Though in low percentage, the presence of NPs was confirmed by Cryo-SEM microphotographs, which depict their presence (data not shown). Moreover, as lower-sized particles are lighter, recovery medium together with centrifugation may not have been completely successful and some particles may have been retained in the emulsified and non-aqueous phase.

Hereupon, as size-fractionation of microgel particles led to unwanted aggregation phenomena, a strategy was searched to minimize particle aggregation and to allow a

427 better ADS particles size characterization. Sonication is routinely included in particle
428 dispersion being applied to produce uniform-sized alginate nanocapsules
429 (Lertsutthiwong, Noomun, Jongaroonngamsang, Rojsitthisak & Nimmannit, 2008) and
430 polyelectrolyte coated NPs (Zheng, Zhang, Carbo, Clark, Nathan & Lvov, 2010). This
431 technique was chosen as an attempt to eliminate or decrease particles' aggregation and
432 therefore to allow a narrower particle size distribution. Two five-minute ultrasonication
433 cycles were performed in the particles-containing suspensions to ascertain its effect on
434 particle size distribution, which was evaluated in separate by size-measurements by LD.
435 Fig. 2(b) shows the size distribution of ADS particles after the first ultrasonication
436 cycle. After this first exposure, insulin particles moved to a predominantly submicron
437 and micron ranges, depicted by a notable deviation to the left of the distribution curve in
438 relation to initial profile in Fig. 2(a), in particular for the nanoscale. This lead to a
439 significant decrease of percentile percentage values as we can see in Table 1, and
440 consequently the percentage of higher-size particles decreased substantially. After the
441 second ultrasonication cycle, there were no significant differences in size distribution
442 behaviour. In this study, there were no differences also between insulin and unloaded
443 particles about size distributions (data not shown). As LD technique allows a wide size
444 range (0.040–2000 μm), exposed to ultrasonication samples, which were previously
445 determined to be in the absence of higher-sized microparticles, were also analysed by
446 Dynamic Light Scattering (DLS). This last technique shows reliable scope analysis up
447 to 1000nm, and the results for ultrasonicated samples were consistent with the results
448 given above by LD, namely 793 ± 71 nm of mean particle size and 0.37 of PI. This
449 confirmed the existence and predominance of NPs in ADS particles populations after
450 ultrasonication. Like in the present experiment, a 30-second ultrasonication cycle of
451 antigen-alginate particles significantly reduced the mean diameter, size range and their
452 percentage over 10μm, but increasing the sonication time, there were no significant
453 changes (Ghiasi, Sajadi Tabasi & Tafaghodi, 2007).
454 Ultrasonication may have disaggregated particles in some extension but there were
455 probably irreversible aggregates that remain unchanged. In turn, span values, in Table 1,
456 were reduced after ultrasonication exposure, confirming once more the enhancement of
457 lower-sized particles after ultrasonication, but it still remains the necessity for
458 optimizing towards nanoscale applications.
459 ADS particles exhibited a roughly spherical shape with smooth surface which is
460 characteristic of these particles (Reis, Ribeiro, Houng, Veiga & Neufeld, 2007), and it

was not altered by ultrasonication exposure, as we can see through Cryo-SEM microphotographs, in Fig. 3. Their qualitative analysis provided by mass spectroscopy confirmed these observations, through the existence of tungsten, used to stain negatively particles (data not shown).

Centrifugation of microgel dispersed in acetate buffer as a strategy to explore particles' size-fractioning revealed unwanted aggregation, which was not prevented or reversed. In this context, ultrasonication approach to decrease aggregation phenomena minimized this obstacle.

3.4. *In vitro* release

Premature insulin release in the stomach can result in acidic and enzymatic degradation, however release in the intestinal mucosa may improve insulin uptake and translocation through the gastrointestinal tract (Woitiski, Neufeld, Ribeiro & Veiga, 2009). Fig. 4 depicts the release profile of ADS particles under simulated gastric and intestinal conditions. At low gastric pH, no insulin was released from ADS particles, however after the transition to intestinal pH, insulin started to be burst released, up to 4 hours, and then it has maintained release profile, achieving a maximum of ~ 75% of cumulative released insulin after 10 hours. The amount of insulin retained within nanoparticles under intestinal simulation may be tightly bound to the alginate nucleus, so a more extensive dissolution for additional release may be needed (George & Abraham, 2006).

These results demonstrate insulin retention within the particles' core during gastric environment. Once in the intestinal tract, encountering neutral pH, the alginate networks forming the NPs' core swell due to deprotonation becoming increasingly permeable to insulin (Woitiski, Neufeld, Veiga, Carvalho & Figueiredo, 2010), releasing it to the medium. Insulin release from ADS particles is pH dependent, with a continuous release profile, indicating ADS particles as an effective controlled delivery system for insulin.

3.5. Physical stability

Physical stability of ADS suspensions was evaluated through zeta potential measurements and sedimentation tests before and after ultrasonication exposure.

Zeta potential values varied between -25.7 and -31.9 mV, and no significant effect of Ultrasonication on zeta potential values was detected, as we can see in Table 1, pointing to the absence of physical stability changes after ultrasonication. Negative zeta potential

values are a result of surface charges, namely anionic alginate and dextran sulphate chains at pH 4.5. and similar results were obtained for microgel made of similar biopolymers (Reis, 2007). ADS particles presented higher stability than alginate-composed nanospheres, because dextran sulfate assembly conferred higher stability to particle matrix due to higher charge density.

The analysis of separation under accelerated conditions is a useful guide in NPs formulation, minimizing on long-term stability testing and allowing an early detection of gravitational sedimentation problems. Insulin ADS particles analysis results, before and after ultrasonication, can be seen in Fig. 5 and Fig. 6, respectively. A similar behaviour for insulin and unloaded particles was observed, so only insulin ADS particles profiles are shown.

The analysis of the transmission profiles of ADS particles revealed a marked change in demixing behaviour before and after ultrasonication treatment. Starting with the analysis of the particles before of the ultrasonication, if it is considered for instance, the position 116 mm (the middle of the cell) in Fig. 5, the first profile was recorded at ~50% being the last profile, at about 90% of transmission, achieved by a fast increase of transmission (as it can be seen from the accumulation of the green last profiles in the top). Around 123 mm position (the bottom of the cell), the transmission percentage sudden drops as a result of the presence of aggregates which had accumulated in the bottom. This is observed since the beginning of the test (represented by the first recorded red profile in the graph), denouncing that these particles easily deposit, representing a characteristic transmission profile of an aggregated sample. With the advance of the centrifugation time, the height of the pellet decreases, indicating that settled particles aggregated with each other after their deposition. This marked demixing behaviour was also observed macroscopically. The initial sample was a homogenous suspension, in which particles were supposedly homogeneously distributed in the suspension. At the end of the sedimentation test, it was observed a clear supernatant at the top and a turbid pellet in the bottom of the cell, results of demixing process, in accordance to the higher final transmission.

Submitting these particles to ultrasonication, samples acquire a characteristic dispersion profile instead of an aggregated one, where particles are smaller, shown in Fig. 6. The same transmission behaviour was shown for the almost whole sample length, with no significant demixing process. Little fluctuations were visible, which indicates a more homogenous sample in size than the previous one. Comparing both transmission

profiles, before ultrasonication, shown in Fig. 5, a higher transmission was occurred because the larger particles showed a higher separation in the same first interval than in after ultrasonication, in Fig. 6, which showed a lower transmission. It had probably occurred also an accumulation of lower-sized particles in the top of the sample, which was no observed before ultrasonication exposure. These were probably lighter particles of lower size that resulted from the breakdown of aggregates by the use of ultrasonication. A reduced accumulation of particles in the bottom was seen in Fig. 6, representing the existence of larger particles; but with remarkable difference of aggregation extent than initial untreated samples as shown in Fig. 5. After ultrasonication sample, it was visible a lower final transmission, shown in Fig. 6, accompanied with a macroscopically bit turbid along the length of the sample when visually inspected after removal from the rotor. These last particles' populations showed slower particles than before ultrasonication one, due to smaller size and/or smaller density difference to the continuous phase (acetate buffer). These results sustain the previous analysis of particles' size, as well as an increased physical stability after ultrasonication relatively to initial conditions in accordance to zeta potential measurements.

When the suspension is not stabilized enough, particles can regroup back after ultrasonication(Reis, Ribeiro, Neufeld & Veiga, 2007). Sedimentation tests of the same ultrasonicated samples were repeated after one week, and no differences were found between «fresh» ultrasonicated ones, shown in Fig. 6, and one-week-after recorded transmission profiles (data not shown). These results suggest that particles maintain its stability for at least one week after ultrasonication treatment.

Thus, zeta potential analysis suggests ADS particles as physically stable systems before and after ultrasonication exposure. These results were complemented by information given by sedimentation tests, indicating that after ultrasonication all samples become even more stable than the previous ones.

3.6. **Protein bioactivity**

Preservation of the structural integrity of a protein drug during manufacture is crucial for its biological efficacy. Thus, the secondary structure of insulin extracted from ADS particles was assessed by measuring the extent of phosphorylation of intracellular AKT, since AKT phosphorylation is a downstream event triggered by the binding of active insulin to its receptors on the cell surface (Elghazi, Balcazar & Bernal-Mizrachi, 2006).

Fig. 7 shows the activity of extracted insulin before and after ultrasonication. Biological activity of insulin extracted from collected particles was between 60-80%.

The remaining low percentage of insulin bioactivity was possibly due to losses during both preparation and recovery since emulsification/internal gelation comprises various steps critical for biological activity stability of insulin. First, during formation of the water/oil (w/o) emulsion, insulin can be affected by the w/o solvent interface. Interfacial adsorption can be followed by unfolding which results in reduced biological activity. Upon emulsification of an aqueous solution of L-aspariginase into an organic solvent a substancial decrease in enzyme activity was reported. Consequently, the contact with lipophilic interfaces provoked denaturation, but insoluble aggregates were not formed (Wolf, Wirth, Pittner & Gabor, 2003).

A slight change of the insulin's secondary structure (native conformation) was found after encapsulation and recovery processes by similar protocols (Reis, Ribeiro, Houng, Veiga & Neufeld, 2007). A possible explanation is that insulin could be linked to particle's polymers network which can alter protein structure, though not representing denaturation or loss of insulin activity.

Previous results obtained with insulin alginate particles prepared by a similar procedure showed that 55% of insulin retained activity quantified by Western Blot, leading to assume that emulsification/internal gelation is capable of retain particles' insulin bioactivity (Reis, Ribeiro, Houng, Veiga & Neufeld, 2007). Therefore, neither the emulsification nor the proposed recovery protocol showed a specific impact on insulin bioactivity.

Another source of inactivation during ADS particles' preparation is cavitation stress as necessary for disaggregation of NPs. Despite cooling, ultrasonication provokes cavitations with local extremes of temperature and radical formation which adversely affect proteins. As we can see in Fig. 7, submicron particles showed no insulin bioactivity alterations after ultrasonication, even exhibiting a larger surface area to volume ratio in comparison to the higher-sized ones predominant in untreated ADS-particles. Ultrasonication employed in the disaggregation of particles is expected to affect insulin integrity. This could be a risk due to the closer localization of the insulin to the particle surface and higher susceptibility to suffer a greater damage in relation to the protein located in the core of the bigger particles. However, like the present results, insulin NPs were prepared by the Layer-by-Layer adsorption of polyelectrolytes after an

ultrasonication for several minutes and no insulin damage was reported (Fan, Wang, Fan & Ma, 2006).

These results suggest the possibility of ultrasonication use in polydisperse particles populations, without the risk of smaller sized particles damage in relation to insulin bioactivity. Thus, insulin ADS particles constitute a carrier with maintenance capacity of encapsulated insulin bioactivity retention after recovery, handling and ultrasonication exposure.

3.7. Circular Dichroism

Preservation of the structural integrity of a protein drug is important for its biological efficacy, so the secondary structure of insulin released from ADS particles was investigated using CD in the far UV region. Results depicted in Fig. 8 show the CD spectra of fresh diluted insulin reference solution (non-encapsulated), and released insulin from ADS particles before and after ultrasonication. Insulin reference solution in PBS at pH 7.4 showed typical bands with two minima at approximately 209 and 222 nm, indicating the presence of major α-helix structure with part of β–sheets.

CD spectrum of released insulin before ultrasonication show that, besides the presence of the major minimum at 209nm, the minor minimum at 222nm decreased significantly in magnitude (appearing only a slight depression), indicating insulin suffered changes in relation to the reference insulin. These results suggest that the secondary structure of insulin (native conformation) after encapsulation into ADS particles and recovery processes was changed. In the process of ADS particles production, it is known that polymers binding may have caused conformational changes to insulin structure, which normally are detected in CD spectra (Wallace, 2009); moreover, the higher exposition of protein to air/liquid or liquid/solid interfaces, like stirring and centrifugation could be factors that have determined these changes.

In released insulin after ultrasonication CD spectrum, 209nm minimum suffered a decrease in magnitude and 222nm minimum has been shifted to 217nm, which points to enhancement of β–sheets proportion. This is in accordance to previous studies, where sonication of proteins with substantial content in helical structure in the native state, like insulin (Jimenez, Nettleton, Bouchard, Robinson, Dobson & Saibil, 2002), caused an increase in β-structure with a concomitant decrease in α-helical structure (Stathopulos, Scholz, Hwang, Rumfeldt, Lepock & Meiering, 2004). In fact, metmyoglobin, showed

that under stress conditions, such as low temperature and high pressure conditions, was only partially unfolded, with a rigid core consisting of helices remaining folded (Matsuo, Sakurada, Yonehara, Kataoka & Gekko, 2007; Meersman, Smeller & Heremans, 2002). In the present experiments, besides the existence of CD spectra changes, it can be concluded, together with the previous *in vitro* experiments results and HPLC-MS analysis, that insulin was not chemically modified but has suffered a substantial conformational change, as it was exposed by handling conditions, namely after production and recovery, and also after ultrasonication.

In both cases, before and after ultrasonication, released insulin suffered conformational changes from helical structures to β–sheets. This phenomenon occurs differently to proteins with predominantly β-features in native CD spectra which show spectral changes upon sonication less pronounced, and there is little apparent change in secondary structure (Jimenez, Nettleton, Bouchard, Robinson, Dobson & Saibil, 2002), which suggests further biological activity analysis (Corrêa & Ramos, 2009; Kelly, Jess & Price, 2005).

Thus, together to *in vitro* biological activity results as well as the presence of no aggregates as confirmed by HPLC-MS, detected changes in insulin secondary structure cannot be considered as meaningful, being common in released peptide and protein samples (Al-Tahami, Oak & Singh, 2010; Zhang et al., 2010) and thus do not representing loss of biological activity.

3.8. HPLC-MS

Insulin is susceptible to several chemical modifications, and the most common reactions that can occur are deamidation, acylation and peptide bond cleavage (Oak & Singh, 2011). Maintaining protein stability during processing is critical in providing safe and efficacious protein therapeutics with long shelf lives (Reis, Ribeiro, Neufeld & Veiga, 2007), so HPLC-MS was applied to determine the stability of insulin. The HPLC-MS chromatograms of reference insulin solution and insulin extracted from ADS particles were similar as shown in Figure 9 (a) and (b), as well as occurred in the case of reference insulin and insulin extracted from ADS particles after ultrasonication exposure (data not shown). HPLC-MS analysis showed that no high molecular weight transformation products were formed, such as covalent dimmers. So, emulsification/internal gelation procedure, recovery protocol and ultrasonication used to reduce ADS particle size don't affect insulin chemical stability.

4. Conclusions

Size-fractioning of microgel obtained by emulsification showed the presence of high percentage of aggregates. Submitting these particles to ultrasonication allowed the transition from a multimodal and polydisperse population to a more homogeneous and less polydisperse population, where the nanometric scale stands, contrary to initial conditions. This behaviour is sustained by the deviation of the size distribution profile from the micrometric range to the nanometric range and the decrease of respective span values. The use of one ultrasonication-cycle in performed conditions was beneficial to reduce aggregation in these particles, without compromising biological insulin activity and colloidal stability. This entails the necessity to size-segregate these populations, in order to homogenize and standardize different obtained populations to attain a specific and physiological action that is not particularly related to a smaller size. Significant recovery yield, insulin content, shape and surface conservation, as well as preservation of bioactivity of insulin were obtained after all recovery and handling, ADS particles recovered by the use of a recovery medium constituted by acetone and acetate buffer coupling to centrifugation constitute a good strategy to obtain particles with reversible aggregation. This phenomenon is reversed in some extent by the use of ultrasonication without biological and physicochemical risks in performed conditions. However, despite ultrasonication is known to have good disaggregation capacities, insulin secondary structural changes were detected in CD spectra, leading to the necessity of further studies by highly sensitive spectroscopic methods, such as deconvolution of synchrotron radiation circular dichroism and fourier transform infrared spectroscopy spectra if quantitative evaluation is required. Moreover, facing the necessity of solvents use to yield ADS particles recovery, the absence of isopropanol and hexane, as in previous studies, is a beneficial factor in relation to health and environmental issues increasing this technique potential implementing. In doing so, further ultrasonication approaches for ADS particles with well-established and reproducible conditions will be desired, to get stable and narrower populations within submicron range. This stage is indispensible since the application of these particles *in vivo* depends on size and polydispersity-dependent factors, namely the recently established protein corona, capable of determine the dissolution profile, interaction and membranes crossing, absorption, distribution, targeting and insulin biological effects.

Acknowledgements

The authors are grateful to Laboratory of Mass Spectrometry (LEM) of the Node CEF/UC integrated in the National Mass Spectrometry Network (RNEM) of Portugal, for the MS analyses; to Professor João Pessoa and Doctor Isabel Correia of Center for Structural Chemistry, IST-UTL, for their kind support on DC; and for L.U.M. GmbH, Germany (Dias de Sousa S.A.) for the availability of LUMisizer® centrifuge and technical support offered in the interpretation of results. The authors would also like to thank Dr. João Casalta-Lopes, for the support in the performance of statistical analysis.

5. Bibliography

Akbar, N., Mohamed, T., Whitehead, D., & Azzawi, M. (2011). Biocompatibility of amorphous silica nanoparticles: Size and charge effect on vascular function, in vitro. *Biotechnol Appl Biochem, 58*(5), 353-362.

Al-Tahami, K., Oak, M., & Singh, J. (2010). Controlled delivery of basal insulin from phase-sensitive polymeric systems after subcutaneous administration: In vitro release, stability, biocompatibility, in vivo absorption, and bioactivity of insulin. *Journal of Pharmaceutical Sciences, 100*(6), 2161-2171.

Chen, X., Wu, W., Guo, Z., Xin, J., & Li, J. (2011). Controlled insulin release from glucose-sensitive self-assembled multilayer films based on 21-arm star polymer. *Biomaterials, 32*(6), 1759-1766.

Cui, X., Hunter, W., Yang, Y., Chen, Y., & Gan, J. (2011). Biodegradation of pyrene in sand, silt and clay fractions of sediment. *Biodegradation, 22*(2), 297-307.

Elghazi, L., Balcazar, N., & Bernal-Mizrachi, E. (2006). Emerging role of protein kinase B/Akt signaling in pancreatic beta-cell mass and function. *Int J Biochem Cell Biol, 38*(2), 157-163.

Fan, Y. F., Wang, Y. N., Fan, Y. G., & Ma, J. B. (2006). Preparation of insulin nanoparticles and their encapsulation with biodegradable polyelectrolytes via the layer-by-layer adsorption. *International Journal of Pharmaceutics, 324*(2), 158-167.

Gan, Q., Dai, D., Yuan, Y., Qian, J., Sha, S., Shi, J., & Liu, C. (2012). Effect of size on the cellular endocytosis and controlled release of mesoporous silica nanoparticles for intracellular delivery. *Biomedical Microdevices, 14*(2), 259-270.

Gaumet, M., Gurny, R., & Delie, F. (2009). Localization and quantification of biodegradable particles in an intestinal cell model: the influence of particle size. *Eur J Pharm Sci, 36*(4-5), 465-473.

Geiser, M., Rothen-Rutishauser, B., Kapp, N., Schurch, S., Kreyling, W., Schulz, H., Semmler, M., Im Hof, V., Heyder, J., & Gehr, P. (2005). Ultrafine particles cross cellular membranes by nonphagocytic mechanisms in lungs and in cultured cells. *Environmental health perspectives, 113*(11), 1555-1560.

George, M., & Abraham, T. E. (2006). Polyionic hydrocolloids for the intestinal delivery of protein drugs: Alginate and chitosan - a review. *Journal of Controlled Release, 114*(1), 1-14.

Ghiasi, Z., Sajadi Tabasi, S., & Tafaghodi, M. (2007). Preparation and In Vitro Characterization of Alginate Microspheres Encapsulated with Autoclaved Leishmania major (ALM) and CpG-ODN. *Iranian Journal of Basic Medical Sciences, 10*(2), 90–98.

743 Hasani, S., Pellequer, Y., & Lamprecht, A. (2009). Selective Adhesion of Nanoparticles
744 to Inflamed Tissue in Gastric Ulcers. *Pharmaceutical Research, 26*(5), 1149-1154.
745 Hirn, S., Semmler-Behnke, M., Schleh, C., Wenk, A., Lipka, J., Schäffler, M.,
746 Takenaka, S., Möller, W., Schmid, G., Simon, U., & Kreyling, W. G. (2011). Particle
747 size-dependent and surface charge-dependent biodistribution of gold nanoparticles after
748 intravenous administration. *European Journal of Pharmaceutics and Biopharmaceutics,*
749 *77*(3), 407-416.
750 Hwang, W. S., Truong, P. L., & Sim, S. J. (2012). Size-dependent plasmonic responses
751 of single gold nanoparticles for analysis of biorecognition. *Analytical Biochemistry,*
752 *421*(1), 213-218.
753 Krishnankutty, R. K., Mathew, A., Sedimbi, S. K., Suryanarayan, S., & Sanjeevi, C. B.
754 (2009). Alternative routes of insulin delivery. *Zhong Nan Da Xue Xue Bao Yi Xue*
755 *Ban,34*(10), 933-948.
756 Lerche, D. (2002). Dispersion Stability and Particle Characterization by Sedimentation
757 Kinetics in a Centrifugal Field. *Journal of Dispersion Science and Technology, 23*(5),
758 699-709.
759 Lertsutthiwong, P., Noomun, K., Jongaroonngamsang, N., Rojsitthisak, P., &
760 Nimmannit, U. (2008). Preparation of alginate nanocapsules containing turmeric oil.
761 *Carbohydrate Polymers, 74*(2), 209-214.
762 Luo, J., Cao, S., Chen, X., Liu, S., Tan, H., Wu, W., & Li, J. (2012). Super long-term
763 glycemic control in diabetic rats by glucose-sensitive LbL films constructed of
764 supramolecular insulin assembly. *Biomaterials, 33*(33), 8733-8742.
765 Nguyen, V. S., Rouxel, D., Hadji, R., Vincent, B., & Fort, Y. (2011). Effect of
766 ultrasonication and dispersion stability on the cluster size of alumina nanoscale particles
767 in aqueous solutions. *Ultrason Sonochem, 18*(1), 382-388.
768 Oak, M., & Singh, J. (2011). Controlled delivery of basal level of insulin from
769 chitosan–zinc–insulin-complex-loaded thermosensitive copolymer. *Journal of*
770 *Pharmaceutical Sciences, 101*(3), 1079-1096.
771 Oliva, A., Farina, J., & Llabres, M. (2000). Development of two high-performance
772 liquid chromatographic methods for the analysis and characterization of insulin and its
773 degradation products in pharmaceutical preparations. *J Chromatogr B Biomed Sci Appl,*
774 *749*(1), 25-34.
775 Poncelet, D., Lencki, R., Beaulieu, C., Halle, J. P., Neufeld, R. J., & Fournier, A.
776 (1992). Production of alginate beads by emulsification/internal gelation. I.
777 Methodology. *Appl Microbiol Biotechnol, 38*(1), 39-45.
778 Reis, C. P. (2007). Encapsulation of peptide drugs by the method of
779 emulsification/internal gelation. *Laboratory of Pharmaceutical Tecnhology of*
780 *University of Coimbra* (p. 620): Coimbra.
781 Reis, C. P., Ribeiro, A. J., Houng, S., Veiga, F., & Neufeld, R. J. (2007).
782 Nanoparticulate delivery system for insulin: design, characterization and in vitro/in vivo
783 bioactivity. *Eur J Pharm Sci, 30*(5), 392-397.
784 Reis, C. P., Ribeiro, A. J., Neufeld, R. J., & Veiga, F. (2007). Alginate microparticles as
785 novel carrier for oral insulin delivery. *Biotechnol Bioeng, 96*(5), 977-989.
786 Reis, C. P., Ribeiro, A. J., Veiga, F., Neufeld, R. J., & Damge, C. (2008).
787 Polyelectrolyte biomaterial interactions provide nanoparticulate carrier for oral insulin
788 delivery. *Drug Deliv, 15*(2), 127-139.
789 Reis, C. P., Veiga, F. J., Ribeiro, A. J., Neufeld, R. J., & Damge, C. (2008).
790 Nanoparticulate biopolymers deliver insulin orally eliciting pharmacological response. *J*
791 *Pharm Sci, 97*(12), 5290-5305.

Silva, C. M., Ribeiro, A. J., Figueiredo, I. V., Goncalves, A. R., & Veiga, F. (2006). Alginate microspheres prepared by internal gelation: development and effect on insulin stability. *Int J Pharm, 311*(1-2), 1-10.

Silva, C. M., Ribeiro, A. J., Figueiredo, M., Ferreira, D., & Veiga, F. (2005). Microencapsulation of hemoglobin in chitosan-coated alginate microspheres prepared by emulsification/internal gelation. *AAPS J, 7*(4), E903-913.

Tiyaboonchai, W., Woiszwillo, J., Sims, R. C., & Middaugh, C. R. (2003). Insulin containing polyethylenimine-dextran sulfate nanoparticles. *International Journal of Pharmaceutics, 255*(1-2), 139-151.

Wissing, S. A., Kayser, O., & Muller, R. H. (2004). Solid lipid nanoparticles for parenteral drug delivery. *Advanced Drug Delivery Reviews, 56*(9), 1257-1272.

Woitiski, C. B., Neufeld, R. J., Ribeiro, A. J., & Veiga, F. (2009). Colloidal carrier integrating biomaterials for oral insulin delivery: Influence of component formulation on physicochemical and biological parameters. *Acta Biomater, 5*(7), 2475-2484.

Woitiski, C. B., Neufeld, R. J., Veiga, F., Carvalho, R. A., & Figueiredo, I. V. (2010). Pharmacological effect of orally delivered insulin facilitated by multilayered stable nanoparticles. *Eur J Pharm Sci, 41*(3-4), 556-563.

Wolf, M., Wirth, M., Pittner, F., & Gabor, F. (2003). Stabilisation and determination of the biological activity of l-asparaginase in poly(d,l-lactide-co-glycolide) nanospheres. *International Journal of Pharmaceutics, 256*(1-2), 141-152.

Zhang, N., Li, J., Jiang, W., Ren, C., Li, J., Xin, J., & Li, K. (2010). Effective protection and controlled release of insulin by cationic β-cyclodextrin polymers from alginate/chitosan nanoparticles. *International Journal of Pharmaceutics, 393*, 213-219.

Zheng, Z., Zhang, X., Carbo, D., Clark, C., Nathan, C., & Lvov, Y. (2010). Sonication-assisted synthesis of polyelectrolyte-coated curcumin nanoparticles. *Langmuir, 26*(11), 7679-7681.

LIST OF FIGURES

Fig. 1 - Optical microphotograph of system droplets during emulsification of manufacture process (1000×). Samples were died with Victoria-blue R.

Fig. 2 – Particle size distribution profile of ADS particles: (a) particles are mainly distributed in the micrometric range, owing to the presence of higher-sized particles and aggregates. (b) After one five-minute cycle of ultrasonication exposure, there was a narrower particle size distribution mainly composed by NPs. The second five-minute cycle of ultrasonication didn't introduce any significant changes.

Fig. 3 – Insulin ADS particles after one sonication-cycle, by Cryo-SEM (25000x, 15kV, WD=15mm). Ultrasonication allows obtaining a low disperse population. Characteristic core-shell shape of these particles is easily observable through 3D visualization.

Fig. 4 – *In vitro* release profile of ADS particles in simulated gastric medium at pH 1.2 followed intestinal medium at pH 6.8, depending on time. Results are means ± SD of three experiments.

Fig. 5 – Recorded evolution (from red to green colour) of time dependent transmission profiles of insulin ADS particles, depicting a characteristic profile of an aggregated sample with clear demixing behaviour. Profiles were taken every 30 s at 2000 rpm during 128 minutes. X-axis represents the position of the rotor.

Fig. 6 – Recorded evolution (from red to green colour) of time dependent transmission profiles of insulin loaded-alginate-dextran sulfate particles after ultrasonication, revealing a characteristic dispersion profile, where particles were smaller and less polydisperse. Profiles were taken every 30 s at 2000 rpm during 128 minutes. X-axis represents the position of the rotor.

Fig. 7 – Bioactivity of insulin contained in ADS particles before and after ultrasonication by FACE™ AKT ELISA assay (mean ± SD; n = 3). ADS particles showed high bioactivity retention, which was maintained after ultrasonication exposure indicated by no significant differences (considering significant difference for *p* value less than 0.05, n=3).

Fig. 8 – CD spectra of insulin in solution (5 μM) in PBS at pH 7.4 and 25°C: (solid line) insulin non-encapsulated (reference solution), (dashed line) insulin released from ADS particles before ultrasonication and (dotted line) insulin released from ADS particles after ultrasonication exposure.

Fig. 9 – HPLC-Mass representative chromatograms of reference solution of: (a) insulin non-encapsulated (reference solution) and (b) insulin released from ADS particles, both before ultrasonication exposure.

868 **Table 1.** Particle Size Analysis and Zeta Potential of ADS particles before and after
869 Ultrasonication Exposure
870

	***d*10% (µm)**	***d*50%(µm)**	***d*90%(µm)**	**Span value**	**Zeta Potential (mV)**
Insulin ADS particles	0.364±0.124	26.16±3.89	144.8±30.45	5.521	-31.9±1.4
1 ultrasonication cycle exposed insulin ADS particles	0.114±0.062	0.352±0.101	1.803±0.182	4.798	-26.2±1.2
2 ultrasonication cycles exposed insulin ADS particles	0.203±0.054	0.425±0.088	2.051±0.167	4.348	-25.7±1.5
Unloaded ADS particles	0.534±0.172	28.53±9.69	164.7±29.94	5.754	-30.3±1.1

871 Diameter values corresponding to percentiles of 10%, 50%, and 90%, zeta potential (mean ± SD,
872 n=3), and span value of insulin ADS particles before and after being exposed to one and two five-
873 minute ultrasonication cycles.
874 [a] Significant difference with a *p* value of less than 0.05 was verified between before and
875 after being exposed to both 1 and 2 ultrasonication cycles.
876 [b] There was no difference between 1 and 2 ultrasonication cycle expositions.
877
878

878 **Highlights**

879 • A recovery protocol was applied to obtain narrower hydrogel particles'
880 populations
881 • Size-fractioning of hydrogel particles shows high aggregation degree
882 • Ultrasonication reverses particles' aggregation and homogenizes populations
883 • Insulin bioactivity is maintained after ultrasonication exposure
884 • Particles dispersed in aqueous medium show good stability after ultrasonication
885
886

Fig. 1 - Black and white.tif

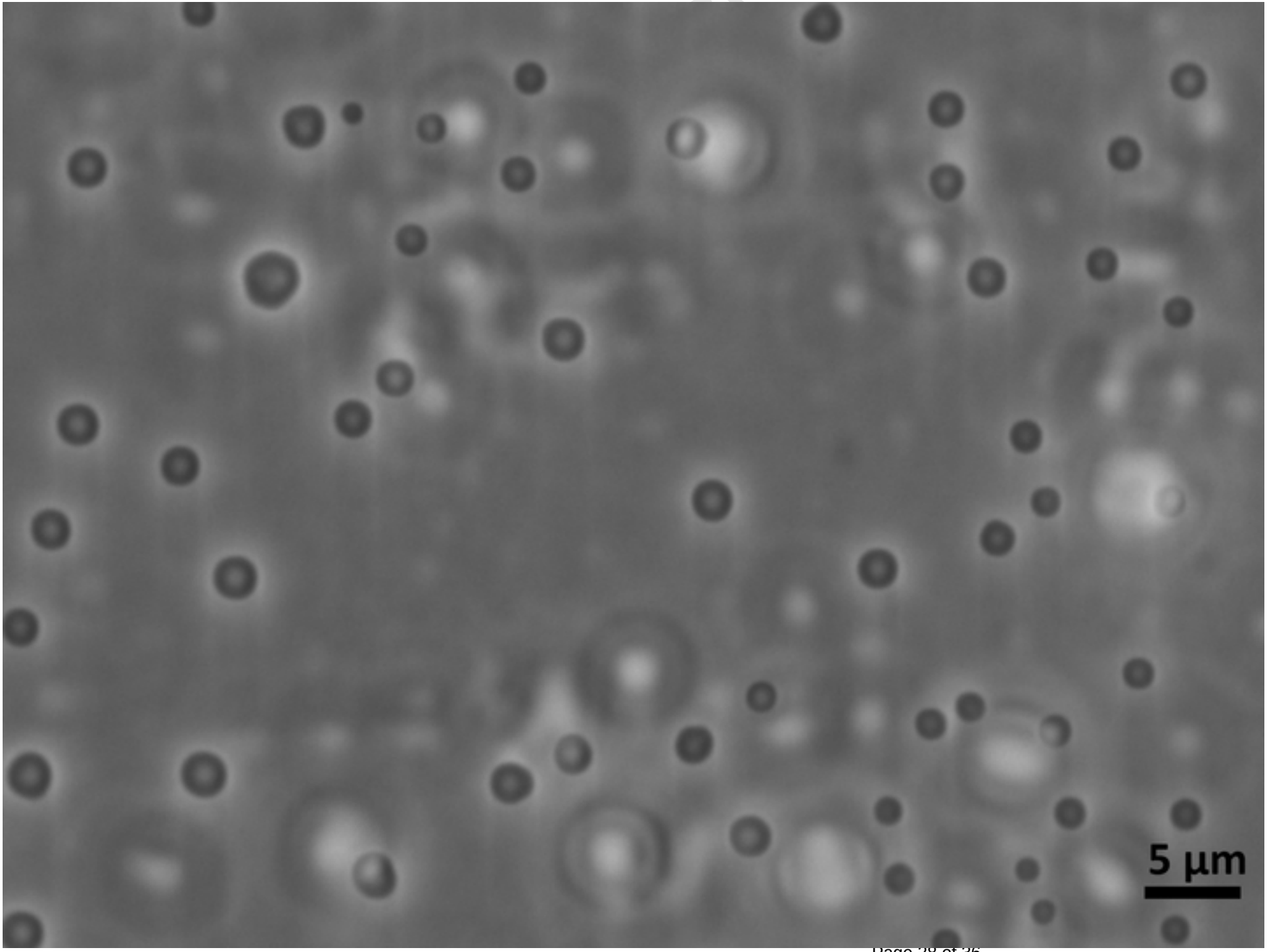

Fig. 2 - Black and white.tif

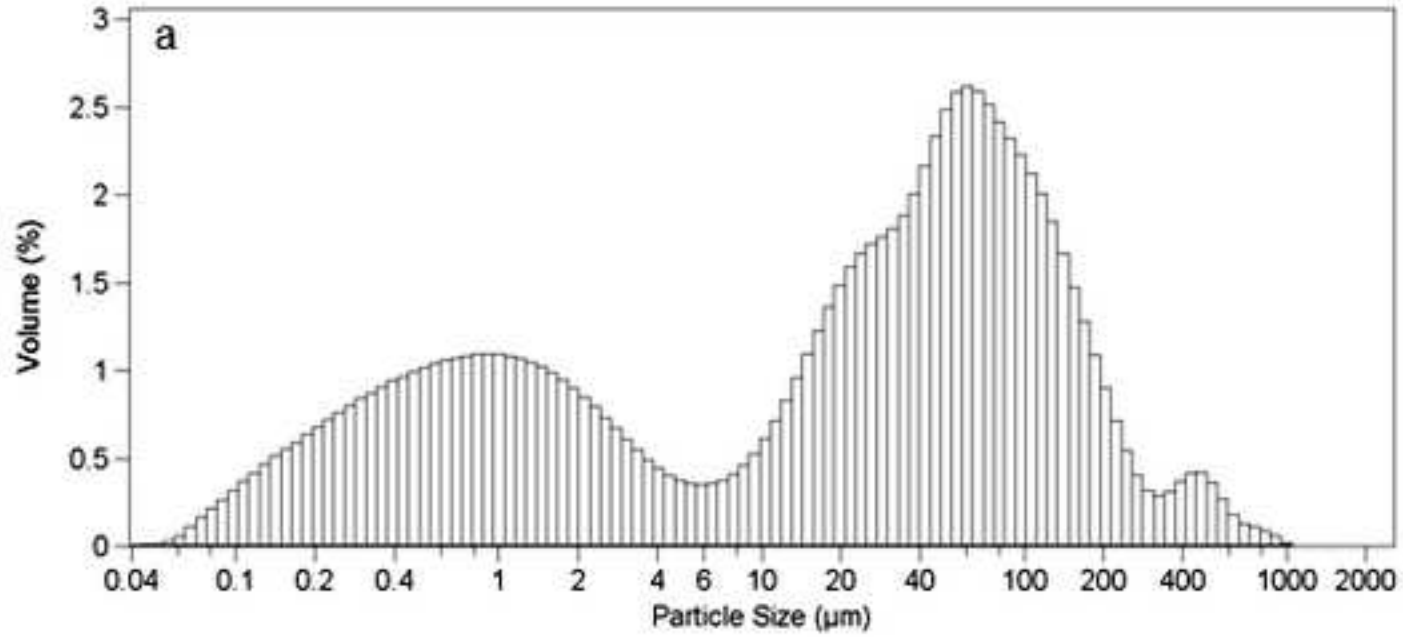

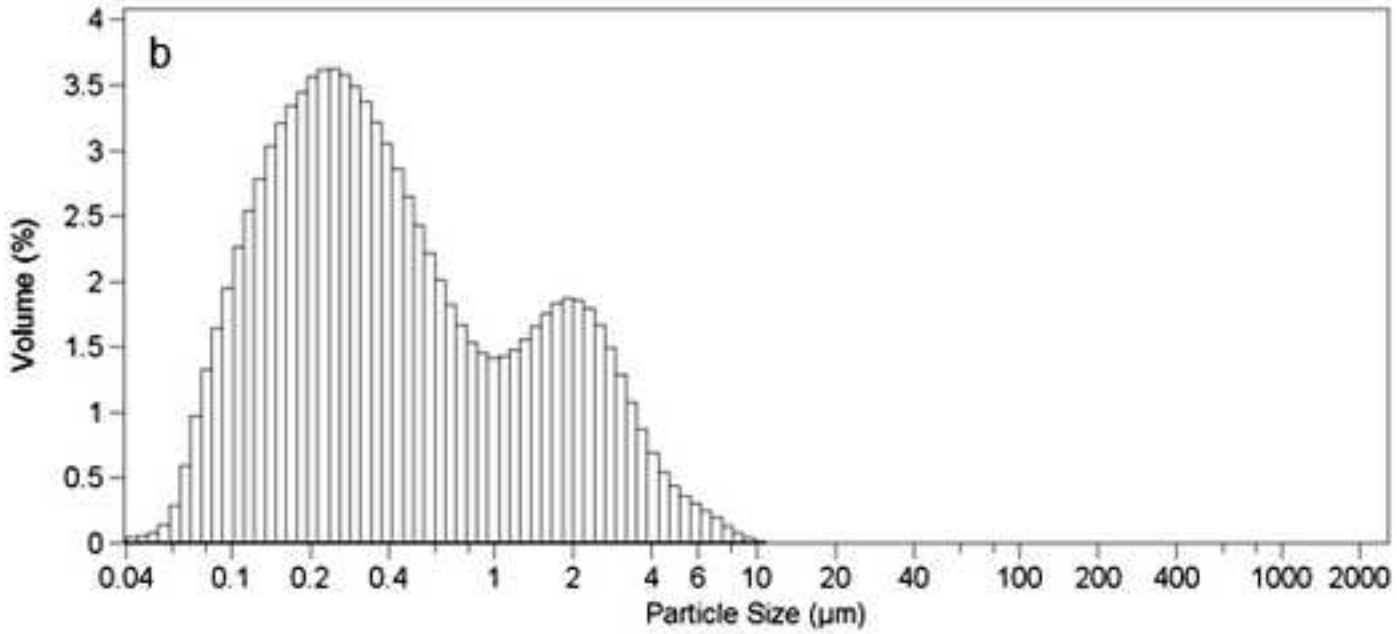

Fig. 3.tif

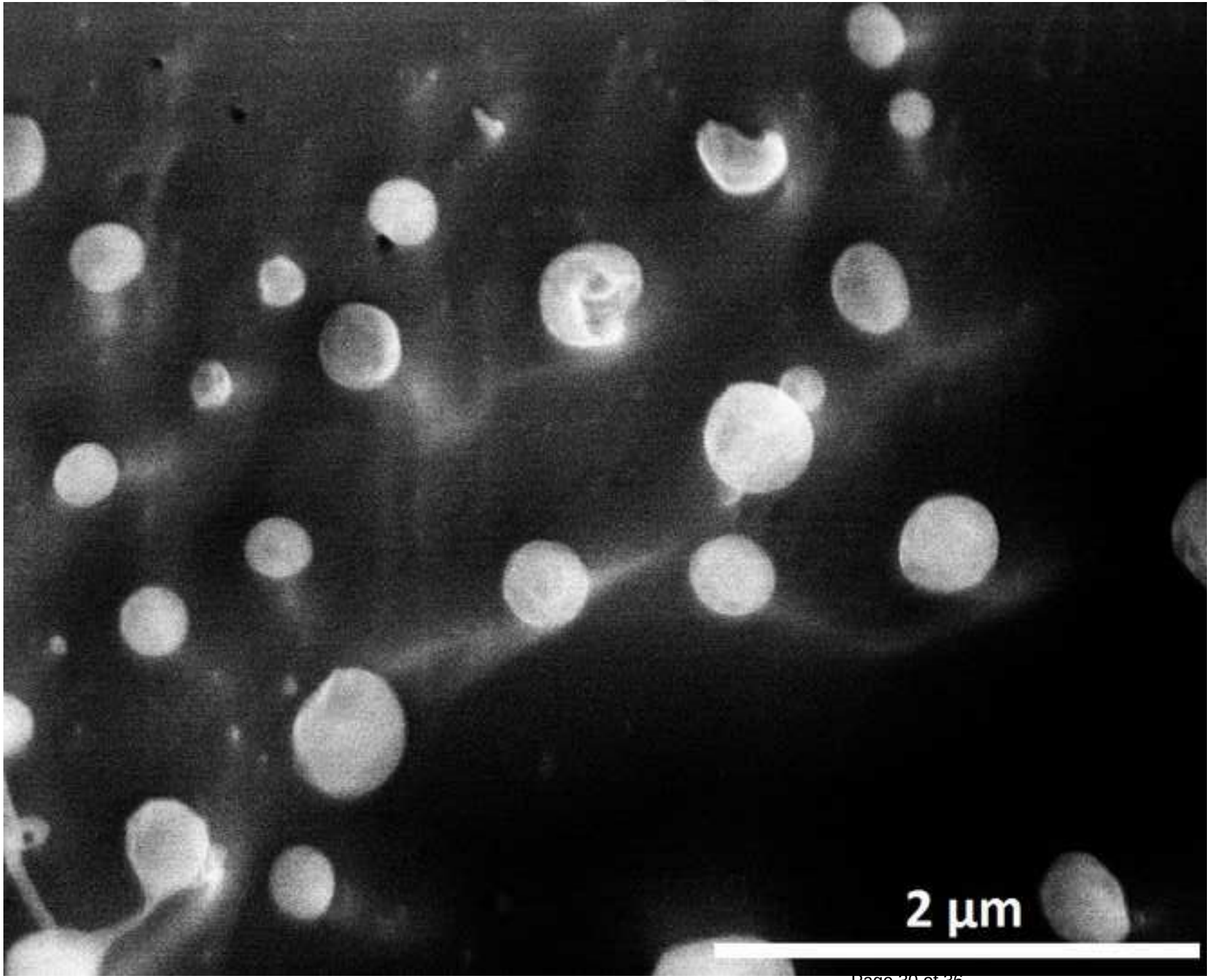

Figure 4

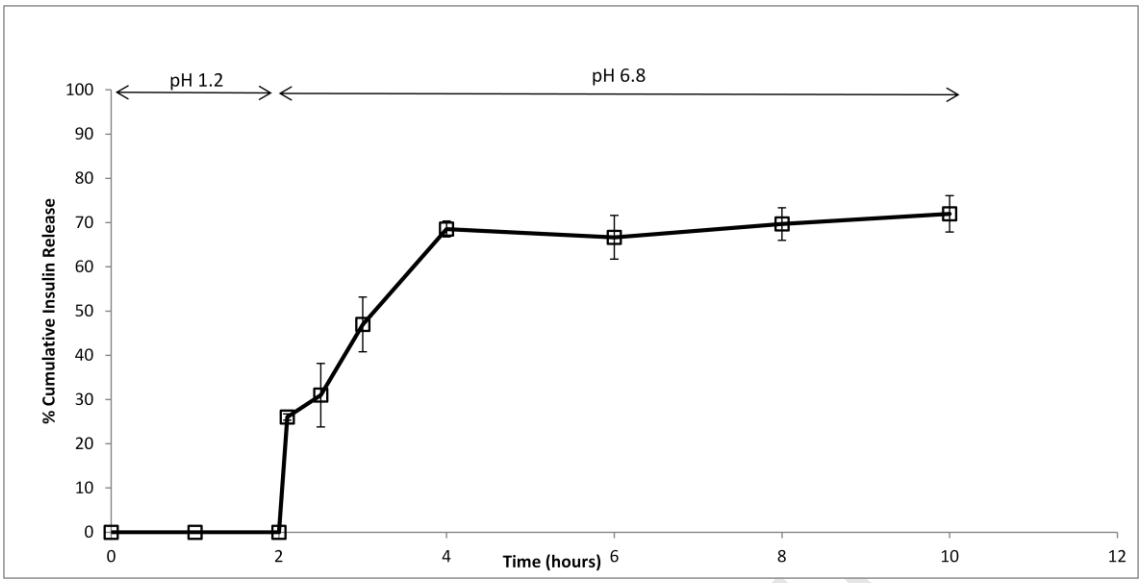

Figure(s)

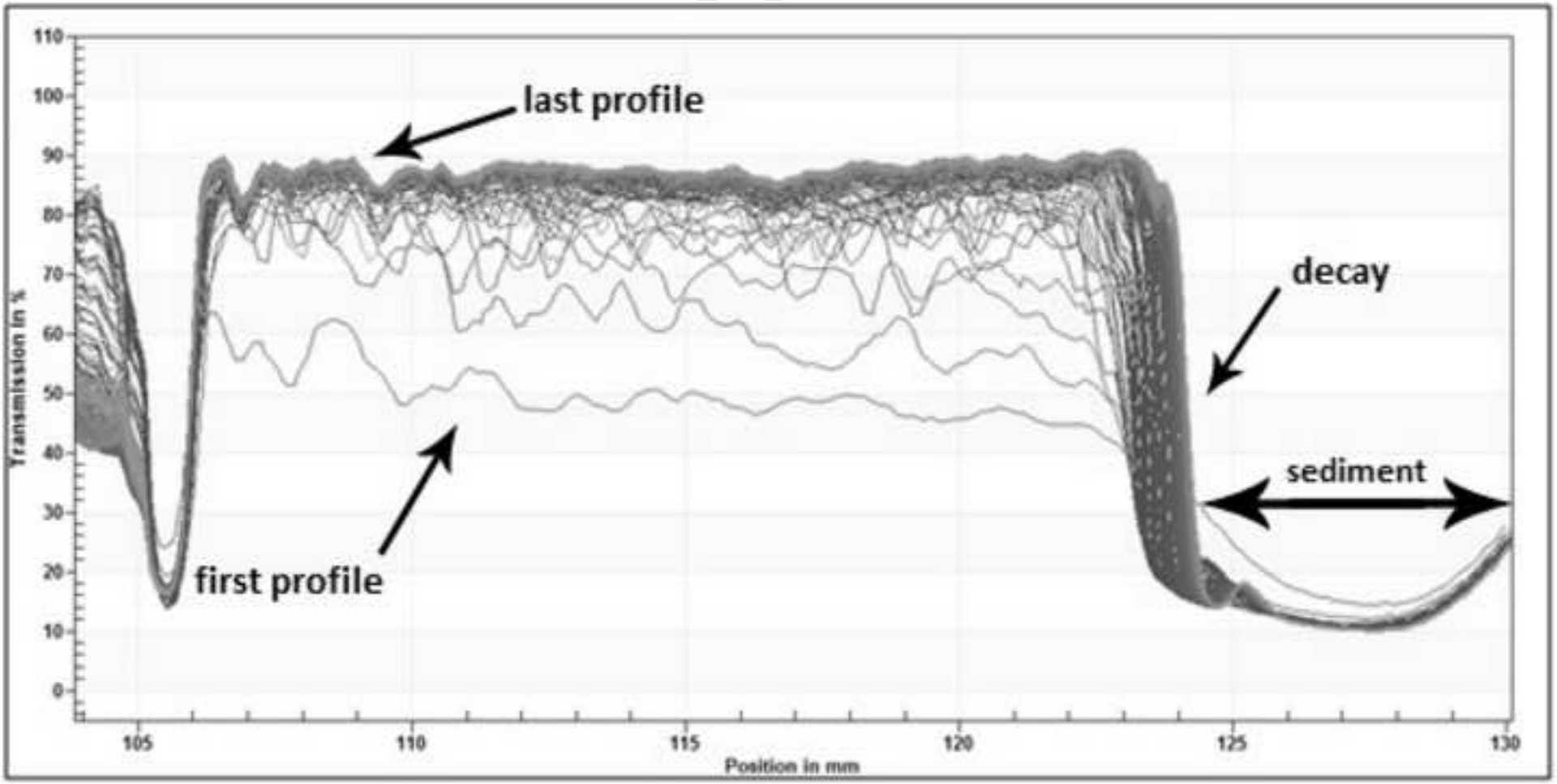
last profile
decay
sediment
first profile
Transmission in %
Position in mm
110
100
90
80
70
60
50
40
30
20
10
0
105
110
115
120
125
130

Figure(s)

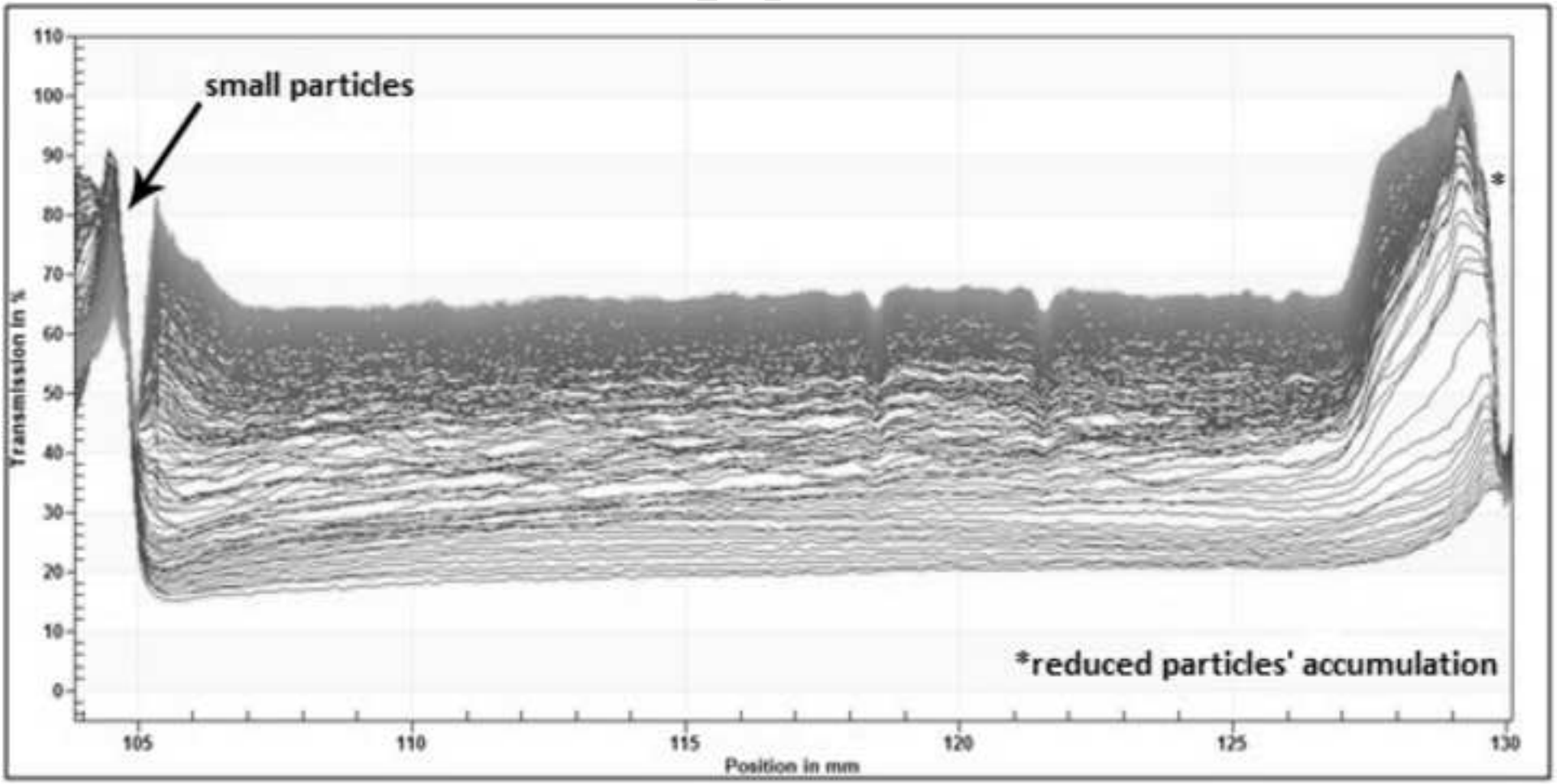
small particles
*
*reduced particles' accumulation
Transmission in %
Position in mm
110
100
90
80
70
60
50
40
30
20
10
0
105
110
115
120
125
130

Figure 7

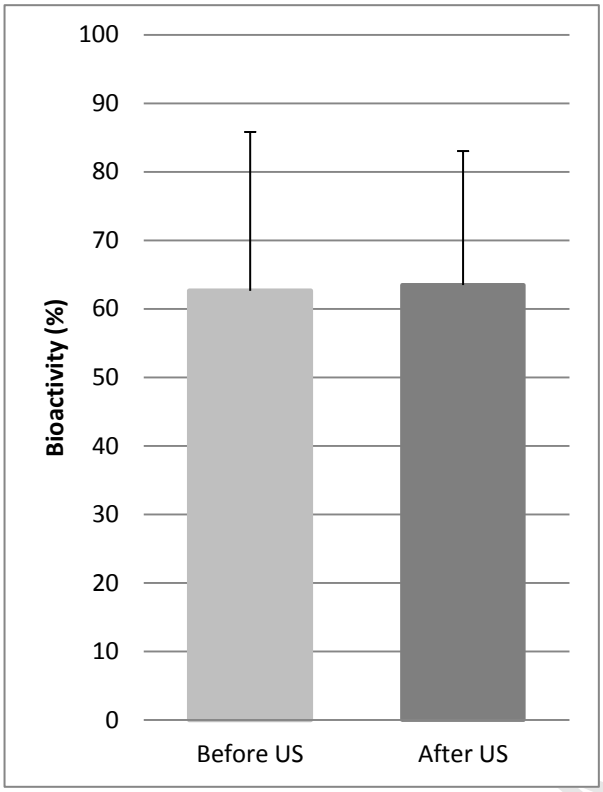

Figure 8